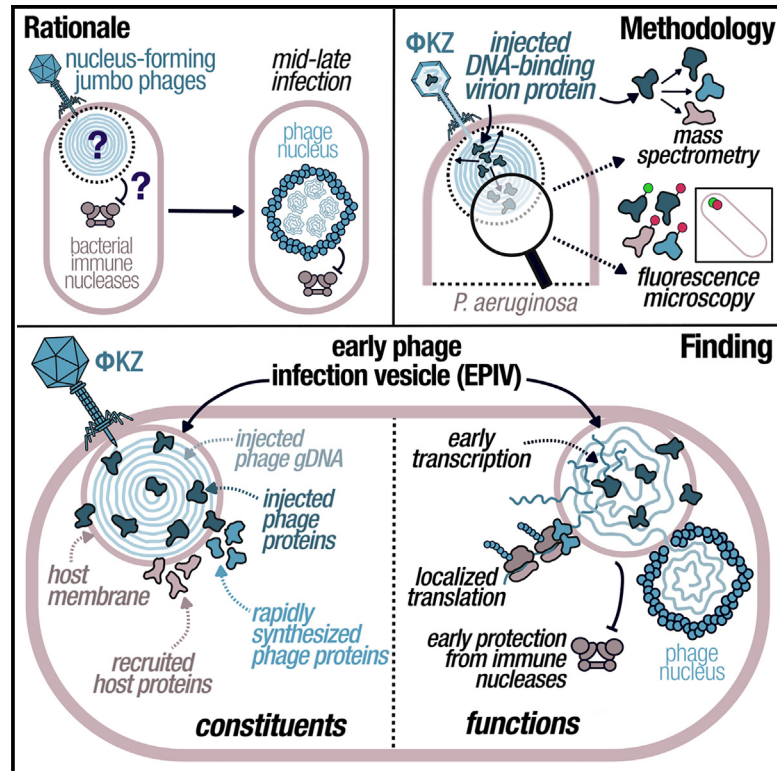# Cell Host & Microbe

Characterization of a lipid-based jumbo phage compartment as a hub for early phage infection

Graphical abstract

Authors

Deepto Mozumdar, Andrea Fossati, Erica Stevenson, ..., David Agard, Danielle L. Swaney, Joseph Bondy-Denomy

Correspondence

joseph.bondy-denomy@ucsf.edu

In brief

Mozumdar et al. describe an early phage infection (EPI) vesicle that is rapidly assembled with injected phage proteins and bacterial membrane components during *Pseudomonas aeruginosa* infection by jumbo phage ΦKZ. Virion RNAP (vRNAP) is deposited inside the vesicle to enable early transcription, whereas phage DNA is protected from immune nucleases.

Highlights

- Host membrane and membrane proteins are rapidly recruited during phage ΦKZ infection

- Host lipids and injected phage proteins assemble a vesicle executing early transcription

- Early-expressed phage proteins are recruited to the vesicle, with some binding ribosomes

- Vesicle protects the injected genome from nucleases prior to phage nucleus assembly

CellPress

Short article

Characterization of a lipid-based jumbo phage compartment as a hub for early phage infection

Deepto Mozumdar,[1] Andrea Fossati,[2,3,4] Erica Stevenson,[2,3,4] Jingwen Guan,[1] Eliza Nieweglowska,[5] Sanjana Rao,[1] David Agard,[5,6] Danielle L. Swaney,[2,3,4] and Joseph Bondy-Denomy[1,3,7,*]

[1]Department of Immunology and Microbiology, University of California, San Francisco, San Francisco, CA 94158, USA
[2]J. David Gladstone Institutes, San Francisco, CA 94158, USA
[3]Quantitative Biosciences Institute (QBI), University of California, San Francisco, San Francisco, CA 94158, USA
[4]Department of Cellular and Molecular Pharmacology, University of California, San Francisco, San Francisco, CA 94158, USA
[5]Department of Biochemistry and Biophysics, University of California, San Francisco, San Francisco, CA 94158, USA
[6]Chan Zuckerberg Imaging Institute, Redwood City, CA 94065, USA
[7]Lead contact
*Correspondence: joseph.bondy-denomy@ucsf.edu
https://doi.org/10.1016/j.chom.2024.05.016

SUMMARY

Viral genomes are most vulnerable to cellular defenses at the start of the infection. A family of jumbo phages related to phage ΦKZ, which infects *Pseudomonas aeruginosa*, assembles a protein-based phage nucleus to protect replicating phage DNA, but how it is protected prior to phage nucleus assembly is unclear. We find that host proteins related to membrane and lipid biology interact with injected phage protein, clustering in an early phage infection (EPI) vesicle. The injected virion RNA polymerase (vRNAP) executes early gene expression until phage genome separation from the vRNAP and the EPI vesicle, moving into the nascent proteinaceous phage nucleus. Enzymes involved in DNA replication and CRISPR/restriction immune nucleases are excluded by the EPI vesicle. We propose that the EPI vesicle is rapidly constructed with injected phage proteins, phage DNA, host lipids, and host membrane proteins to enable genome protection, early transcription, localized translation, and to ensure faithful genome transfer to the proteinaceous nucleus.

INTRODUCTION

ΦKZ-like jumbo phages infecting *Pseudomonas*, *Serratia*, *E. coli*, *Vibrio*, and *Salmonella* build a large proteinaceous nucleus-like compartment[1,2] that houses the replicating bacteriophage DNA and selectively excludes diverse DNA-targeting bacterial immune nucleases.[3,4] The compartment itself is constructed of a large protein lattice made up of a single protein called PhuN or Chimallin subunit A (ChmA),[5,6] encoded as gp54 in phage ΦKZ.[2] This structure is centered in the cell by a tubulin-like protein called PhuZ,[7] where the nucleus often grows larger than the width of the cell during phage DNA replication. The phage encodes DNA polymerase and a non-virion RNA polymerase (nvRNAP) complex,[8–10] which are presumed to be responsible for replication and transcription, respectively, inside the nucleus-like structure.[1] Phage mRNAs are exported from the phage nucleus likely via RNA-binding shell protein ChmC[11] and are translated in the cytoplasm, whereas some phage and host proteins are imported into the phage nucleus.[1] Capsid and tail assembly proceeds in the cytoplasm and the phage DNA is loaded at the phage nucleus periphery where capsids dock to receive the phage genome.[1,7] Throughout these latter stages of infection, the phage genome is therefore completely protected from host nucleases[3,4] and displays remarkable viral organization, akin to virus factories assembled by eukaryotic viruses.

Despite generally strong knowledge about the middle and late stages of infection,[1–4,7,12] the early stages remain poorly defined. ΦKZ requires both the type IV pilus[13] and flagellum[14] to initiate infection in *Pseudomonas aeruginosa* (*P. aeruginosa*), leading to apparent injection at the pole.[12,14,15] ΦKZ packages and ejects a virion RNAP (vRNAP) complex[9,16] along with its genome, which initiates rapid transcription. The major phage nucleus protein (PhuN/ChmA) is rapidly transcribed and translated to assemble and protect the phage genome during replication, but it is not built until ~20–30 min post infection.[1,17] How the injected genome is protected from immune nucleases and what its surroundings are shortly after injection is currently unknown. We have previously presented two lines of evidence that the phage DNA is protected from nucleases by an entity distinct from the phage nucleus: (1) ΦKZ resists endogenous and overexpressed restriction enzymes and clustered regularly interspaced short palindromic repeats (CRISPR) enzymes that act quickly during infection, suggesting that the injected DNA is not immediately exposed for degradation,[3] (2) upon infection arrest via Cas13a-induced depletion of the transcript encoding PhuN/ChmA, phage DNA was stably present in the cell for >1 h despite the presence of an active type I restriction-modification system.[3]
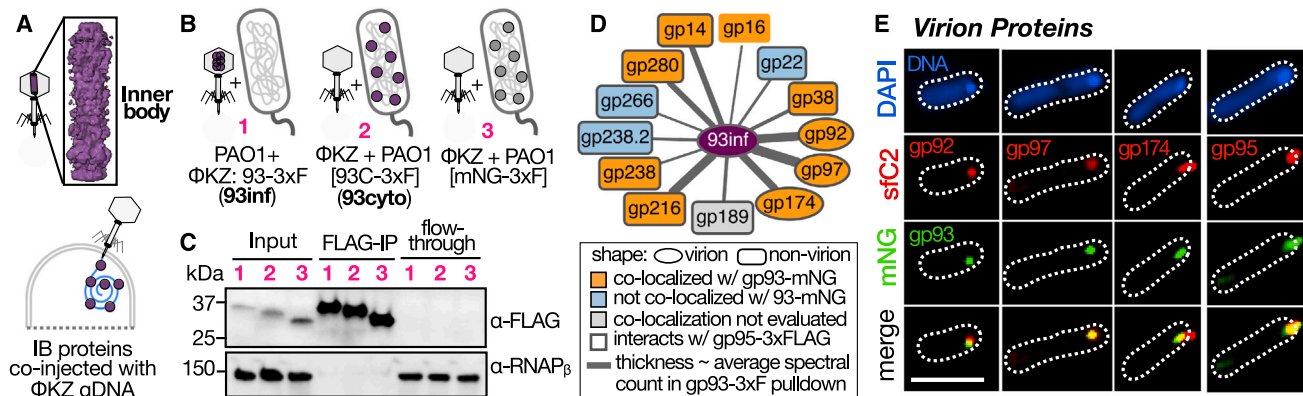
Figure 1. AP-MS with inner body protein gp93-3xFLAG reveals the proteinaceous constituents of a putative early structure

(A) During infection, the proteinaceous inner body[22,23] of ΦKZ is co-injected into bacterial cells with the phage genomic DNA.

(B) Cartoon schematic illustrating the setup of the FLAG AP-MS experimental samples, namely, (1) PAO1 cells infected with ΦKZ: gp93-3xFLAG (93inf), (2) PAO1 cells expressing an N-terminal truncated gp93C-3xFLAG infected with ΦKZ (93cyto), or (3) mNeonGreen-3xFLAG infected with ΦKZ.

(C) Representative α-FLAG western blot of 3xFLAG-tagged protein levels from MS samples in cellular lysate input, FLAG-IP and flow-through. α-RNAPβ is used as a loading control.

(D) Interactome map of ΦKZ proteins that are detected in AP-MS with BFDR < 0.05 in 93inf compared with mNG-3xF and 93cyto-negative control. Gray border: protein-protein interaction (PPI) was also found at high confidence (BFDR ≤ 0.05) with phage-injected gp95.

(E) Representative fluorescence microscopy images of PAO1 cells infected with ΦKZ: gp93-mNeonGreen (mNG; green) packaged with gp92/95/97/174-sfCherry2 (sfC2; red). Cells stained with DAPI (4',6-diamidino-2-phenylindole) to visualize DNA. Scale bars, 5 μm.

See also Figure S1 and Table S1 and Data S1.

Following these observations, thin-section transmission electron microscopy studies observed that ΦKZ (infecting *P. aeruginosa*) and a related phage SPN3US (infecting *S. typhimurium*) generate small round organelles early in the infection.[17,18] More recent studies have observed that cells infected with 201Φ2-1 phage (*P. chlororaphis*) or Goslar phage (*E. coli*) possess "unidentified spherical bodies (USBs)" or "early phage infection (EPI) vesicles," which were proposed to contain a lipid bilayer based on cryo-electron tomography (cryo-ET).[6,19] The function and constituents of this early organelle, whether it derives from the host inner membrane, and whether injected phage DNA or protein are inside, remain unclear.

To understand the processes that ensure faithful early infection, we sought to identify host and phage proteins that associate with the injected phage genome. To do this, we turned to proteins injected into the cell with the phage genome. The "inner body" (IB) is a large cylindrical proteinaceous structure in the phage head[20–23] (Figure 1A). A previous mass spectrometry (MS) study with tailless virions reported six highly abundant virion proteins (gp89, 90, 93, 93, 95, 97, and 162) that likely constitute the majority of this IB structure.[23] Although little is known about these proteins, we have previously shown that gp93 is a non-essential protein that is packaged in the virion and deposited in the cell with the phage genome.[15] Additionally, our previous work using unbiased size exclusion chromatography-MS (SEC-MS) and immunoblotting demonstrated seven additional proteins (gp95, gp97, gp94, gp153, gp163, gp177, and gp184) that are also injected into the cell during infection.[24] However, the localization of these proteins during injection are unknown. Here, we image some of these injected proteins and use them as bait to identify the host and phage constituents of an early organelle that appears immediately at the start of infection. The injected protein and DNA cargo of ΦKZ-like jumbo phages associates with lipids derived from the bacterial membrane to form a lipidic compartment distinct from the protein-based nucleus, which is a hub for early phage infection biology.

RESULTS

The injected protein gp93 of ΦKZ interacts with host metabolic and membrane proteins

To reveal the early environment proximal to the phage genome early in the infection, we selected proteins to use as bait for affinity-purification MS (AP-MS) experiments. Given the high gp93 protein copy number in the virion,[23] clear evidence of injection into the host,[15,24] and the previous biochemical observation that gp93 associates with the phage genomic DNA,[23] it was chosen as one bait protein. To determine the localization of other IB proteins during infection, wild-type (WT) ΦKZ was propagated on strains expressing fluorescently labeled proteins to allow for their packaging. Then labeled virions were used to infect naive cells expressing no fluorescent protein. This revealed that gp89, gp90, gp93, gp95, gp97, and gp162 are, indeed, all packaged into the virion, but only gp90, gp93, gp95, and gp97 are injected (Figure S1A). Interestingly, although gp90 and gp97 had a similar localization pattern to gp93 (i.e., associated with the injected DNA and subsequent migration with the phage nucleus), gp95 appeared to dissociate from the phage nucleus as it matured. We therefore selected gp95 as a second protein to use for AP-MS because it may reveal distinct information. Interestingly, bioinformatics analysis of the IB proteins revealed that gp93, gp95, gp97, gp162, and gene neighbors gp92, gp94, and gp163 all share a paralogous domain (PF12699.11) and are proteolyzed during packaging,[23] suggesting that these participate in a shared, but currently unknown, functionality (Figures S1B and S1C). We next assessed what gp93 and gp95 interactors can reveal about the environment the ΦKZ genome finds itself in shortly after the start of infection.
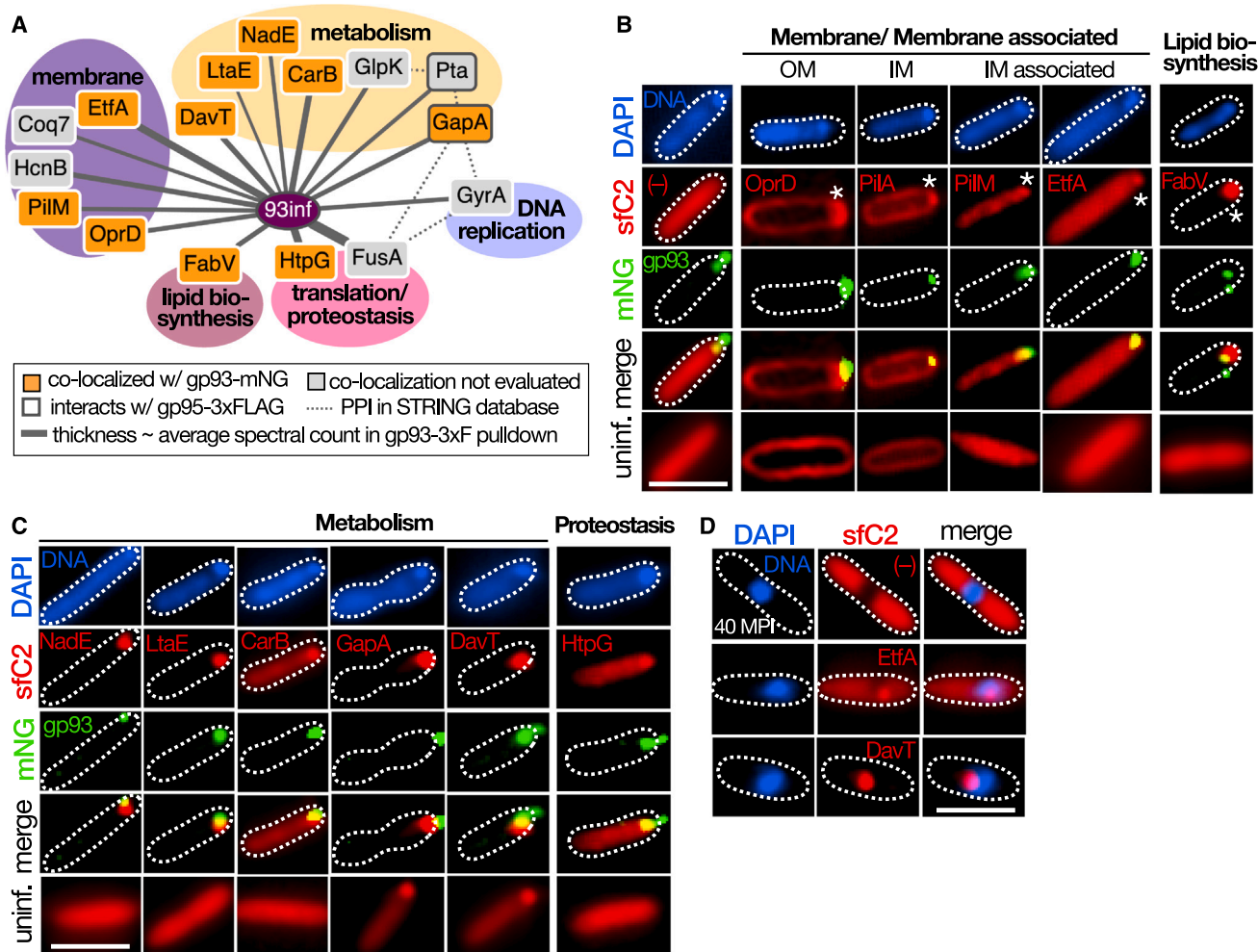
Figure 2. The injected protein cargo of ΦKZ interacts with host metabolic, chaperone, and membrane proteins

(A) Interactome map of PAO1 host proteins that are detected in AP-MS with BFDR < 0.05 in 93inf samples compared with mNG-3xF and 93cyto-negative control. Line style: solid line are interactions derived from gp93 AP-MS experiments. Dotted lines are prey-prey connections derived from the STRING database (all types of connections with STRING score ≥ 0.5).

(B and C) Representative fluorescence microscopy images of PAO1 cells expressing C-terminal sfCherry2 (sfC2) fusions of host proteins associated with (B) bacterial membrane/membrane biogenesis functions or (C) metabolism or proteostasis functions, infected with ΦKZ: gp93-mNeonGreen (mNG) for 10 min.

(D) Representative fluorescence microscopy images of PAO1 cells expressing C-terminal sfCherry2 fusions of host proteins that localize to the phage nucleus at 40 min post infection (MPI).

(B–D) Cells stained with DAPI to visualize DNA. Scale bars, 5 μm. (B) OM, outer membrane; IM, inner membrane.

See also Table S2 and Data S1.

To identify gp93 interactors, gp93 with a C-terminal 3xFLAG affinity tag was packaged into the phage virion to conduct affinity purification during infection ("gp93inf") and subsequent MS analysis. Interactors that were specifically enriched in the injected gp93 purification were assessed by comparing the detected protein intensities with experiments in which gp93-3xFLAG was expressed in the cytoplasm (i.e., not entering the cell from the phage virion, "gp93cyto") and to an mNeonGreen (mNG)-3xFLAG-negative control (Figure 1B). An injected gp95-3xFLAG ("gp95inf") experiment was also performed in parallel. Infections were arrested with gentamicin to limit *de novo* synthesis and synchronize the protein harvest time point. This preferentially captures proteins injected from the phage or recruited from the host, as opposed to proteins synthesized in response to

phage infection. Western blotting was used to confirm that the 3xFLAG constructs were expressed and pulled down via FLAG-IP at equivalent levels (Figure 1C). A total of 29 proteins were identified as high-confidence interactors of injected gp93, consisting of 13 phage proteins (Table S1) and 16 host proteins (Table S2). gp93 interactors fell into three groups: virion proteins (Figure 1D, oval), non-virion phage proteins (Figure 1D, rounded rectangle), and host proteins (Figure 2A). Most of the phage proteins that interact with gp93 also appeared to interact with injected gp95, when the same AP-MS experiment was conducted (Figure 1D, gray outline); however, gp93 and gp95 did not appear as interactors. One explanation for these results is that these paralogous proteins may compete for binding to the same complex of injected proteins.

Prior work has demonstrated that the ΦKZ virion consists of up to ~80 different virion proteins.[23,24] Of this list, three virion phage proteins gp92, gp97, and gp174 (Figure 1D, oval) appeared as gp93/gp95 interactors during infection (but not in gp93cyto) and are likely co-injected with gp93/gp95 and phage genomic DNA (gDNA). To confirm that these proteins are packaged into the phage virion, we propagated ΦKZ with mNG-gp93 tagged endogenously in the phage genome (ΦKZ::gp93-mNG)[15] on strains expressing C-terminal sfCherry2 fusions to enable packaging. Phages grown in this manner were then used to infect PAO1 expressing no fluorescent proteins, which revealed that the queried proteins were, indeed, injected (Figure 1E). Both gp97 and gp92 showed colocalization with gp93, whereas gp174 showed only partial colocalization (Figure 1E). These data provide validation for the AP-MS approach yielding proteins that are co-injected with gp93/gp95 and the phage DNA. However, we did not identify gp93/gp95 interactions with paralogs present in the virion at low copy[23] (gp94 and gp163), perhaps due to their low abundance.

Many gp93 interactors are *Pseudomonas* host proteins associated with metabolism and bacterial membranes/lipids (Figure 2A). Note that this interactome is specific to the injected gp93 and not observed with cytoplasmic gp93. To investigate the possible recruitment of these proteins to the injected DNA and protein, we fused a C-terminal sfCherry2 to the host proteins and evaluated their localization in uninfected cells and cells infected for 10 min with ΦKZ::gp93-mNG (Table S2). We observed a clear relocalization of several cytosolic and membrane proteins to the point of infection (Figures 2B and 2C). We observed recruitment of host proteins that are found either within or associated with the bacterial membrane (OprD, PilM, EtfA, and PilA) to the injected phage gDNA and gp93-mNG (Figure 2B) along with a protein involved in fatty acid biosynthesis, FabV (Figure 2B). Interestingly EtfA and DavT stayed affiliated with the mature phage nucleus later in the infection, at 40 min post infection (MPI) (Figure 2D). With respect to these host proteins, injected gp95 only showed an interaction with Pta and GapA but not other gp93 interactors (Figure 2A, gray outline), likely because gp95 appears to dissociate from the phage gDNA-protein complex early in the phage infection cycle (Figure S1A). Together, these data reveal membrane proteins associating with injected phage protein tightly associated with phage DNA and suggest that membrane recruitment or remodeling may be enacted early during phage infection.

The injected phage genome and protein cargo of ΦKZ are associated with a lipid rearrangement

Given the high number of cell envelope and membrane proteins being recruited to the gp93-phage DNA complex, we next sought to directly investigate if, indeed, the early part of the infection cycle is accompanied by the rearrangement of membrane lipids to the injected phage gDNA and protein cargo. To visualize the potential recruitment of lipids to the injected phage gDNA, we used fluorescence microscopy to track the localization of lipids using the lipophilic dye FM4-64, while staining total DNA using DAPI staining. FM4-64 is a dye that has been used to label endocytic compartments in eukaryotic cells.[25] In phage infections arrested with gentamicin, we observed that the injected phage gDNA localizes as intense DAPI-stained puncta just inside the cell envelope (Figure 3A, blue). Interestingly, with FM4-64 staining, in addition to the

expected labeling of the bacterial membrane, we observed intense punctate staining colocalized with the injected ΦKZ gDNA (Figure 3A, red and overlay). We observed similar FM4-64 stained puncta colocalized with the injected phage DNA in infections of another nucleus-forming jumbo phage ΦPA3 (Figure 3A). Moreover, ΦKZ infections arrested with Cas13a-targeting transcripts encoding the major nucleus protein gp54 (Figure 3B) revealed a similar staining pattern, suggesting that lipid re-arrangements precede nucleus formation. FM4-64-stained puncta are not observed in samples of uninfected cells (Figures 3A and 3B), nor do DNA-containing ΦKZ or ΦPA3 virions in a cell lysate stain positive with FM4-64 (Figure 3C).

We next tracked the localization of the injected phage protein gp93, along with the injected gDNA and FM4-64-stained polar puncta. In gentamicin-arrested infections of ΦKZ::gp93-mNG, we observed that the gp93-mNG packaged in the phage virion is co-injected with the phage gDNA and co-localizes with the FM4-64-stained puncta just inside the cell (Figure 3D). Notably, while observing sequential stages of phage cargo ejection in independent cells, (Figure 3D, 1–3) we observed that the FM4-64 staining was most prominent when both the phage gDNA and gp93-mNG appeared to be completely injected into the bacteria (Figure 3D, 3). To confirm the membrane staining results, a distinct dye was used (1-(4-trimethyl ammoniumphenyl)-6-phenyl-1,3,5-hexatriene p-toluenesulfonate) (TMA-DPH), which is membrane permeable unlike FM4-64. Using this dye, we observed a similar pattern of accumulation of membrane stain (blue) at the site of injection colocalized with the injected gp93-mNG (Figure 3E). Overall, these results suggest that bacterial membranes are recruited to the injected phage gDNA and protein cargo of ΦKZ-like jumbo phages during the early parts of the phage infection cycle. Based on the collective evidence from fluorescence microscopy experiments and previous cryo-ET,[6,19] we suggest that the injected phage gDNA and protein cargo associate with lipids derived from the bacterial inner membrane to assemble a small spherical compartment. To be consistent with previous work,[19,26] we refer to this body as the EPI vesicle.

The EPI vesicle is distinct from the phage nucleus

The phage nucleus is bound by protein[5,6] and not by membrane,[1] but it is unclear what the spatiotemporal relationship is between the phage DNA, the EPI vesicle, and the proteinaceous phage nucleus. To address this, infections were allowed to progress for 40 min, during which the phage nucleus would assemble, and the DAPI-stained phage DNA would move to the middle of the cell due to the tubulin-like protein PhuZ. The FM4-64-stained puncta largely disappear at later time points, but in a small percentage of cells, the FM4-64 stained puncta were observed, where they remained at the cell pole (Figure 3F). In an attempt to limit movement of the phage nucleus and perhaps stabilize the staining of the EPI vesicle, cells were next infected with a ΔphuZ mutant ΦKZ phage,[15] which limits the movement of the phage nucleus away from the cell pole, but otherwise progresses through infection normally. PAO1 cells were infected with this mutant and stained with FM4-64 and DAPI (Figure 3F) or stained in addition to expressing the major phage nucleus protein PhuN/Chimallin fused to mNG-gp54 (Figure 3G). Indeed, the ΔphuZ mutant phage infection revealed FM4-64 stained puncta just inside the cell envelope, distinct
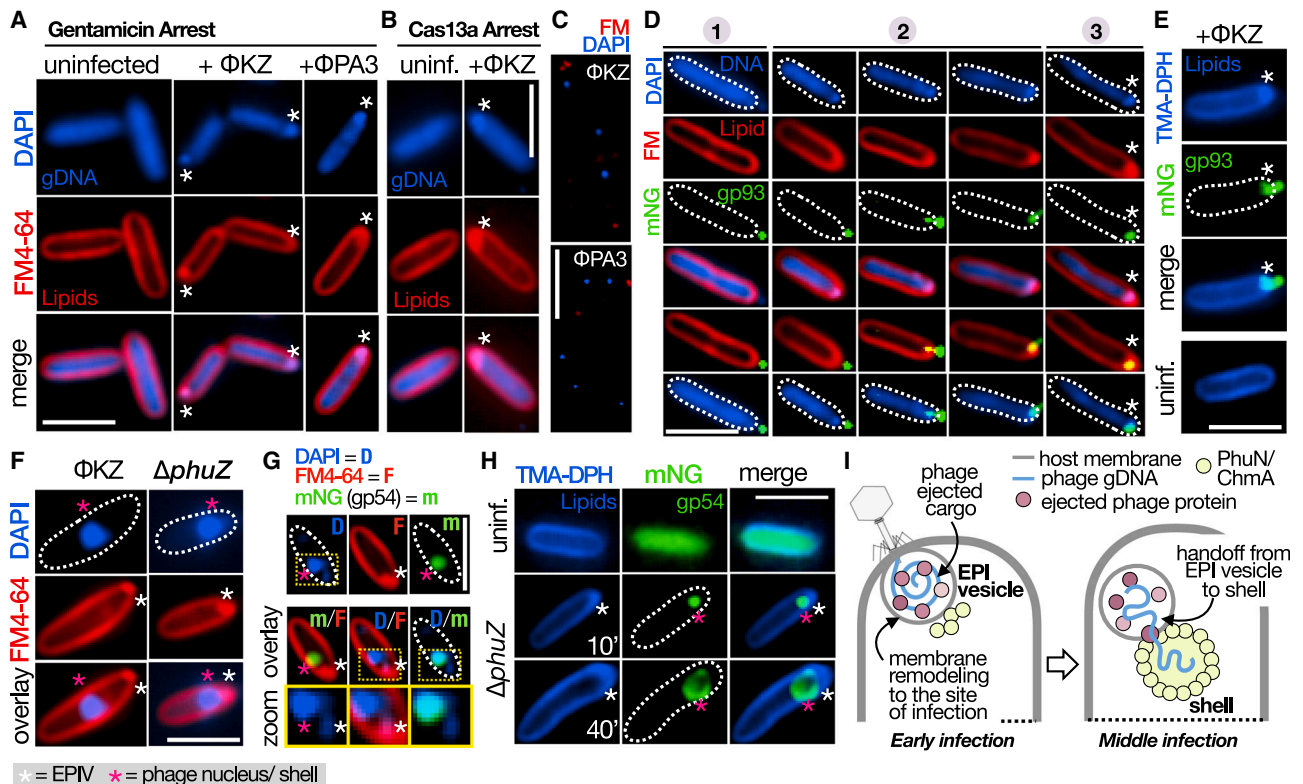
Figure 3. The injected gDNA and protein cargo of ΦKZ-like jumbo phages associates with bacterial-membrane-derived lipids to produce a lipidic compartment distinct from the phage nucleus

(A and B) Representative fluorescence microscopy images of PAO1 cells: (A) treated with gentamicin (50 μg/mL) uninfected/infected with ΦKZ/ΦPA3 or (B) expressing Cas13a and crRNA targeting the transcript of the major ΦKZ nucleus protein gp54; uninfected/infected with ΦKZ.

(C) Representative fluorescence microscopy images of ΦKZ/ΦPA3 virions isolated from bacterial cell lysate stained with DAPI and FM4-64.

(D and E) (D) Representative fluorescence microscopy images of PAO1 cells treated with gentamicin (50 μg/mL) and infected with ΦKZ: gp93-mNeonGreen (mNG). Numbers indicate sequential stages of gp93-mNG and gDNA cargo ejection from phage or (E) uninfected/infected with ΦKZ: gp93-mNG.

(F) Representative fluorescence microscopy images of PAO1 cells infected with WT ΦKZ/PhuZ KO ΦKZ for 40 min.

(G) Representative fluorescence microscopy images of PAO1 cells expressing mNG-gp54 infected with PhuZ KO ΦKZ for 25 min. Middle panel, overlay of indicated channels from top panel; lower panel, zoomed-in-view highlighted in DAPI channel, top panel (yellow rectangle).

(H) Representative fluorescence microscopy images of PAO1 cells expressing mNG-gp54 infected with PhuZ KO ΦKZ for 10 or 40 min.

(A, B, D, F, and G) Cells or (C) virion samples stained with DAPI to visualize DNA and FM4-64 to visualize lipids.

(E and H) Cells stained with TMA-DPH to visualize lipids.

(A, B, and D–H) Asterisks (*): white, EPI vesicle (EPIV); pink, phage nucleus/shell. Scale bars, 5 μm. gDNA, genomic DNA; mNG, mNeonGreen; FM, FM4-64; uninf, uninfected cells.

(I) Model for the EPI vesicle compartment and its relationship to the phage nucleus.

from and adjacent to the DAPI-stained phage DNA inside the mNG-labeled phage nucleus (Figures 3F and 3G). We orthogonally confirmed that the EPI vesicle and phage nucleus form spatially separated compartments by infecting PAO1 cells expressing mNG-gp54 with ΦKZ Δ*phuZ* mutant and staining with lipophilic dye TMA-DPH (Figure 3H). Overall, we propose that the EPI vesicle is independent of the gp54-defined proteinaceous nucleus, which proximally receives the phage DNA in a protected manner in the middle stages of the infection once the nascent phage nucleus has formed (Figure 3I).

The EPI vesicle is a hub for early phage transcription and translation but not DNA replication

For the EPI vesicle to be a productive step in early phage biology, we reasoned that early parts of the ΦKZ infection cycle must be carried out here. These biological processes would include im-

mediate protection from nucleases, phage RNA transcription, mRNA export into the cytoplasm, and protein translation prior to the DNA hand off to the nascent phage nucleus. These statges of the phage life cycle will be queried below.

Early phage RNA transcription is kickstarted immediately after infection by the injected vRNAP complex (constituted by gp80, 149, 178, and 180[9,27]). To assess whether the vRNAP is injected with the phage genome and co-localizes with the EPI vesicle, we packaged ΦKZ with C-terminal sfCherry2 fusions of vRNAP proteins gp149 or gp180. Upon infecting PAO1 cells with these phages, we observed that, indeed, these proteins are co-injected with the phage gDNA (Figure 4A). Interestingly at 40 MPI, we observed that although the replicating phage gDNA appeared in the mature nucleus at the mid-cell position, the vRNAP proteins continued to be observed at the cell pole (Figures 4A and S3A). This pattern is similar to vRNAP localization
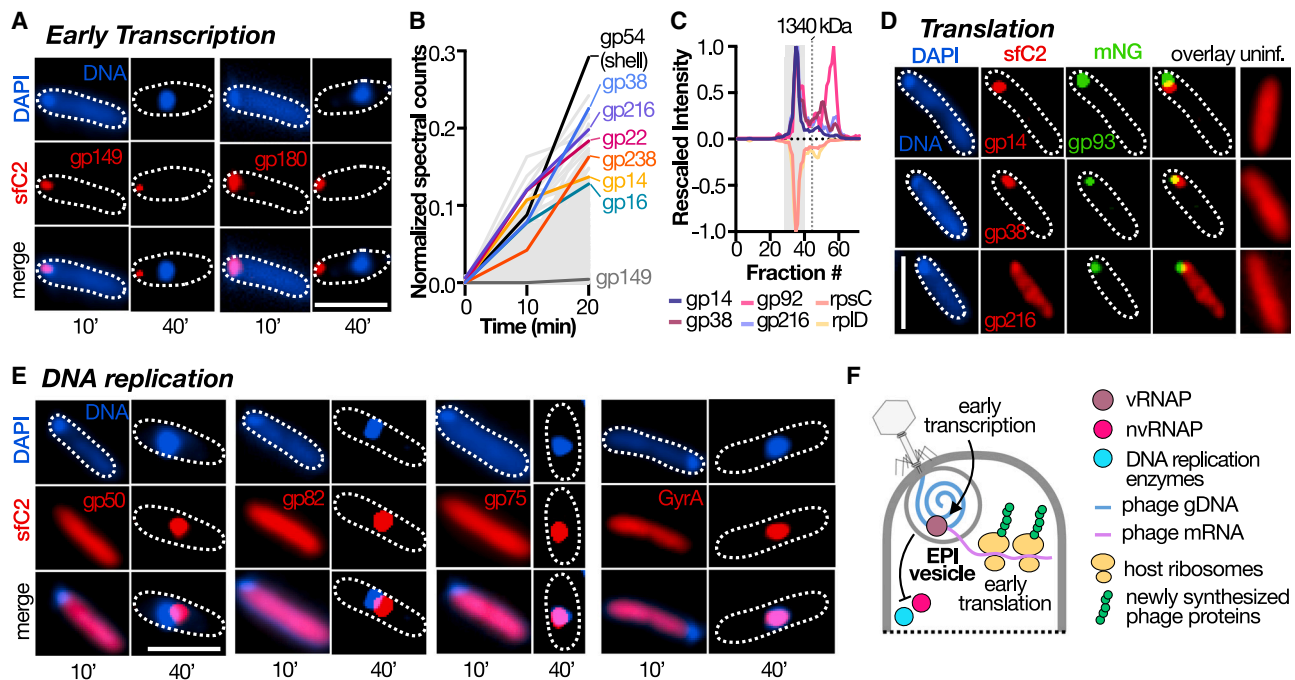
Figure 4. Multiple early phage life cycle functions are carried out at the EPI vesicle

(A) Representative fluorescence microscopy images of PAO1 cells infected for 10 or 40 MPI with ΦKZ packaged with C-terminal sfCherry2 fusions of ΦKZ vRNAP subunits.

(B) Line plot of normalized spectral counts (y axis) vs. time (x axis) of all phage proteins in PAO1 cells infected with ΦKZ. Abundantly synthesized phage proteins detected in gp93-3xFLAG AP-MS are highlighted. Spectral counts of gp54 (major nucleus protein of ΦKZ) and gp149 (vRNAP subunit) shown for comparison.

(C) Elution profiles of PAO1 ribosomal proteins (negative y-axis) and ΦKZ proteins (positive y-axis) that co-elute with the ribosome as determined by SEC-MS.[24] Major peak corresponding to 70S ribosomal assembly highlighted with gray rectangle.

(D) Representative fluorescence microscopy images of PAO1 cells expressing C-terminal sfCherry2 (sfC2) fusions of ribosome associating phage proteins (gp14, 38, and 216) uninfected/infected with ΦKZ:gp93-mNG.

(E) Representative fluorescence microscopy images of PAO1 cells expressing C-terminal sfCherry2 (sfC2) fusions of phage proteins involved with DNA polymerase/helicase functions or PAO1 type II topoisomerase GyrA, uninfected/infected with ΦKZ for 10 or 40 MPI.

(F) Model for the phage life cycle functions carried out within the EPI vesicle. Scale bars: 5 μm in (A), (D), and (E). mNG, mNeonGreen; sfC2, sfCherry2; uninf, uninfected cells.

See also Figures S2–S4.

(gp180) recently also shown to be injected but subsequently left behind as the DNA moves to the nucleus[16] but in stark contrast to the localization of the injected IB proteins (Figure S1A), which move with the phage nucleus. These distinct localization patterns for injected vRNAP and IB proteins could explain why we did not observe vRNAP interacting with gp93 via AP-MS. Additionally, the vRNAP is present in low abundance, estimated at ~10 copies per virion.[16] From these observations, we conclude that the injected phage vRNAP initiates early transcription in the EPI vesicle and is stripped off the phage genome during a regulated transfer of gDNA from the EPI vesicle to the proteinaceous nucleus.

After rapid phage transcription, translation of phage proteins begins. Despite the effective gentamicin arrest (i.e., the phage infection did not progress), some early-expressed phage proteins (gp14, 16, 22, 38, 216, 238, and 280) were also detected as interactors of gp93 (Figure 1D). These proteins have not previously been detected in the virion[23,24]; thus, we suggest that they are highly translated and synthesized during gentamicin treatment. Consistent with this, during unarrested infection, MS revealed that the expression levels of these early proteins are very high, at levels comparable with the most abundantly ex-

pressed phage protein gp54, the major nucleus protein (Figure 4B; Table S1). A subset of the rapidly synthesized phage proteins (namely, gp014, gp038, and gp216) and one injected protein (gp92, Figure 1E) enriched in the gp93inf-MS also associate with the ribosome[24,28] (Figure 4C). Using fluorescence microscopy, we evaluated the subcellular localization of C-terminal sfCherry2 fusions of the phage proteins gp14, gp38, and gp216 expressed in PAO1 cells (Figure 4D). Although these proteins remain diffuse in their localization in uninfected cells, in infected cells, they are rapidly recruited to the site of infection within 10 MPI (Figure 4D). The observation of ribosome-associated phage proteins interacting with injected gp93 and localizing to the EPI vesicle suggests the recruitment of ribosomes to execute localized translation. This is consistent with a cryo-ET observation that proposed polysome accumulation adjacent to the *E. coli* phage Goslar EPI vesicle.[19] A pertinent question that remains unclear is how the phage mRNA is exported from the lipid enclosure of the EPI vesicle to the cytosol to access ribosomes. The remaining rapidly synthesized proteins that associate with gp93 via AP-MS (gp16, 22, 238, and 280) are of unknown function, but gp16 and gp280 appear to be recruited to the site of

infection, whereas gp22 and gp238 form polar puncta prior to phage infection (Figure S4). At 40 MPI, gp238, gp16 and gp280 form strong puncta adjacent to the phage nucleus (Figure S4). Overall, our gp93 AP-MS and previous SEC-MS together with data presented here suggest that specific phage proteins associate with both the EPI vesicle and host ribosomes to potentially facilitate localized translation.

Lastly, we examined proteins that are expected to engage with phage DNA. DNA polymerases/helicases have not been identified in virion proteomes.[23,24] Therefore, the proteins needed for phage DNA replication are expected to be produced *de novo* in the cytosol and must be internalized into either the EPI vesicle or the phage nucleus. DNA replication for ΦKZ starts ~20 MPI.[17] We therefore tracked the subcellular localization of sfCherry2-fusions of phage-encoded DNA replication proteins (DNA polymerase: gp50, gp82; DNA helicase: gp75) expressed in PAO1 cells with respect to the phage gDNA that is injected (10 MPI) or in the nucleus (40 MPI) (Figure 4E). Unlike the host and phage proteins that are rapidly recruited to the EPI vesicle, when examining infected cells at 10 MPI, we observe that the putative DNA replication proteins remain diffuse cytosolic (Figure 4E). Similarly, four different immune system proteins (HsdR, EcoRI, Cas3, and Cas8) are also excluded from the EPI vesicle, as observed with the sfCherry alone negative control (Figure S2A). These data collectively support previous hypotheses that phage DNA is not exposed early in the infection.[3] Later in the infection, when imaged at 40 MPI, phage-encoded (gp50, gp75, and gp82) and host-encoded GyrA (selected because it is a gp93 interactor) DNA replication proteins are recruited to be inside or adjacent to the phage nucleus (Figure 4E). This approximate time point is where host TopA has previously been shown to localize inside the nucleus[1,3] while immune enzymes are excluded.[3] GyrA is the second host protein, together with TopA, known to localize inside the phage nucleus. Our observations indicate that phage gDNA replication is compartmentalized to the phage nucleus, not the EPI vesicle. Collectively, our results establish the EPI vesicle as a hub for early phage transcription and local translation but not for DNA replication or immune nuclease activity (Figure 4F).

DISCUSSION

The selectively permeable nucleus-like compartment assembled by ΦKZ-like jumbo phages to resist DNA-targeting bacterial immune systems represents the most potent anti-immune mechanism discovered to date.[3,4] However, this structure is not built until ~20–30 MPI, and the molecular mechanisms that endow a broad spectrum of protection[3] in early infection have remained elusive. Herein, we report that in the early stages of infection of ΦKZ, a phage-directed EPI vesicle made of bacterial membrane and host proteins is assembled together with injected phage DNA and proteins. The function of this body is to coordinate early transcription and translation processes while protecting the genome from host nucleases.

Our proteomic investigations employed abundant injected virion protein paralogs gp93 and gp95 to query the environment of the phage gDNA. Using these proteomic handles, we observed a similar repertoire of phage protein interactors. However, unique to injected gp93 (i.e., not seen with cytoplasmic

gp93 or injected gp95) were several host proteins associated with bacterial membranes, type IV pilus assembly, membrane biogenesis, and metabolism. Although these proteins suggested a role for recruited membrane, the importance or role of these host proteins in the phage life cycle are not currently known. Subsequent investigations with two lipophilic dyes revealed a strong accumulation of lipid staining at the site of infection consistent with bacterial membrane remodeling. This observation supports independent reports using cryo-ET demonstrating small circular bilayers during infection with diverse jumbo phages,[6,19,26] but having mostly unknown constituents. These observations collectively suggest a phage-driven remodeling of the bacterial membrane to generate an EPI vesicle encapsulating the injected gDNA and protein cargo of ΦKZ-like jumbo phages. Notably this macromolecular compartment is entirely distinct from the phage nucleus in terms of their enclosures (membrane vs. protein) and their function (i.e., early transcription in the EPI vesicle and DNA replication and middle/late transcription in the protein nucleus). Collectively, the two compartments isolate the ejected and replicating phage gDNA from immune nucleases throughout the infection cycle. Our proteomic investigations also identify multiple ribosome-associated phage proteins that may help facilitate mRNA export and/or localized translation at the EPI vesicle. The mechanism of mRNA and DNA export from the EPI vesicle remains a significant open question along with the roles of the many injected protein paralogs (i.e., gp92, gp93, gp94, etc.; Figure S1) and recruited host proteins.

Taken together, our studies reveal the molecular "parts-list" of components that constitute the EPI vesicle, observed in infections of ΦKZ and other related jumbo phages,[6,19,26] and help explain the diverse functions mediated by this compartment. The collective observation that this phage is creating a vesicle analogous to what follows receptor-mediated endocytosis in eukaryotic viruses represents a paradigm in mechanisms employed by bacteriophages to defend against bacterial immune systems in the early parts of the infection cycle where they are most vulnerable to attack.

STAR★METHODS

Detailed methods are provided in the online version of this paper and include the following:

- KEY RESOURCES TABLE
- RESOURCE AVAILABILITY
  - Lead contact
  - Materials availability
  - Data and code availability
- EXPERIMENTAL MODEL AND SUBJECT DETAILS
  - Bacterial strains and phages
- METHOD DETAILS
  - Preparation of phages packaged with fluorescent protein (FP)-labeled phage virion protein
  - Fluorescence microscopy and imaging
  - Western Blotting
  - FLAG AP-MS
  - Time Course MS
  - SEC-MS
  - Bioinformatic Analysis
- QUANTIFICATION AND STATISTICAL ANALYSES
- ADDITIONAL NOTES

AUTHOR CONTRIBUTIONS

Conceptualization, D.M. and J.B.-D.; methodology, D.M., A.F., J.G., D.A., D.L.S., and J.B.-D.; validation, D.M., A.F., J.G., and D.L.S.; formal analysis, D.M., A.F., J.G., E.N., D.L.S., and J.B.-D.; investigation, D.M., A.F., J.G., E.S., S.R., and D.L.S.; resources, D.A., D.L.S., and J.B.-D.; data curation, D.M., A.F., J.G., D.L.S., and J.B.-D; writing—original draft, D.M. and J.B.-D.; writing—review & editing, D.M., A.F., E.N., D.L.S., D.A., and J.B.-D.; visualization: D.M. and D.L.S.; supervision: D.A., D.L.S., and J.B.-D.; project administration, D.M. and J.B.-D.; funding acquisition, D.M., D.A., D.L.S., and J.B.-D.

DECLARATION OF INTERESTS

REFERENCES

1. Chaikeeratisak, V., Nguyen, K., Khanna, K., Brilot, A.F., Erb, M.L., Coker, J.K.C., Vavilina, A., Newton, G.L., Buschauer, R., Pogliano, K., et al. (2017). Assembly of a nucleus-like structure during viral replication in bacteria. Science 355, 194–197. https://doi.org/10.1126/science.aal2130.

2. Chaikeeratisak, V., Nguyen, K., Egan, M.E., Erb, M.L., Vavilina, A., and Pogliano, J. (2017). The Phage Nucleus and Tubulin Spindle Are Conserved among Large Pseudomonas Phages. Cell Rep. 20, 1563–1571. https://doi.org/10.1016/j.celrep.2017.07.064.

3. Mendoza, S.D., Nieweglowska, E.S., Govindarajan, S., Leon, L.M., Berry, J.D., Tiwari, A., Chaikeeratisak, V., Pogliano, J., Agard, D.A., and Bondy-Denomy, J. (2020). A bacteriophage nucleus-like compartment shields DNA from CRISPR nucleases. Nature 577, 244–248. https://doi.org/10.1038/s41586-019-1786-y.

4. Malone, L.M., Warring, S.L., Jackson, S.A., Warnecke, C., Gardner, P.P., Gumy, L.F., and Fineran, P.C. (2020). A jumbo phage that forms a nucleus-like structure evades CRISPR-Cas DNA targeting but is vulnerable to type III RNA-based immunity. Nat. Microbiol. 5, 48–55. https://doi.org/10.1038/s41564-019-0612-5.

5. Nieweglowska, E.S., Brilot, A.F., Méndez-Moran, M., Kokontis, C., Baek, M., Li, J., Cheng, Y., Baker, D., Bondy-Denomy, J., and Agard, D.A. (2023). The φPA3 phage nucleus is enclosed by a self-assembling 2D crystalline lattice. Nat. Commun. 14, 927. https://doi.org/10.1038/s41467-023-36526-9.

6. Laughlin, T.G., Deep, A., Prichard, A.M., Seitz, C., Gu, Y., Enustun, E., Suslov, S., Khanna, K., Birkholz, E.A., Armbruster, E., et al. (2022). Architecture and self-assembly of the jumbo bacteriophage nuclear shell. Nature 608, 429–435. https://doi.org/10.1038/s41586-022-05013-4.

7. Chaikeeratisak, V., Khanna, K., Nguyen, K.T., Sugie, J., Egan, M.E., Erb, M.L., Vavilina, A., Nonejuie, P., Nieweglowska, E., Pogliano, K., et al.

8. Mesyanzhinov, V.V., Robben, J., Grymonprez, B., Kostyuchenko, V.A., Bourkaltseva, M.V., Sykilinda, N.N., Krylov, V.N., and Volckaert, G. (2002). The genome of bacteriophage phiKZ of Pseudomonas aeruginosa. J. Mol. Biol. 317, 1–19. https://doi.org/10.1006/jmbi.2001.5396.

9. Ceyssens, P.-J., Minakhin, L., Van den Bossche, A., Yakunina, M., Klimuk, E., Blasdel, B., De Smet, J., Noben, J.-P., Bläsi, U., Severinov, K., and Lavigne, R. (2014). Development of Giant Bacteriophage φKZ Is Independent of the Host Transcription Apparatus. J. Virol. 88, 10501–10510. https://doi.org/10.1128/JVI.01347-14.

10. Prichard, A., Lee, J., Laughlin, T.G., Lee, A., Thomas, K.P., Sy, A.E., Spencer, T., Asavavimol, A., Cafferata, A., Cameron, M., et al. (2023). Identifying the core genome of the nucleus-forming bacteriophage family and characterization of Erwinia phage RAY. Cell Rep 42, 112432. https://doi.org/10.1016/j.celrep.2023.112432.

11. Enustun, E., Armbruster, E.G., Lee, J., Zhang, S., Yee, B.A., Malukhina, K., Gu, Y., Deep, A., Naritomi, J.T., Liang, Q., et al. (2024). A phage nucleus-associated RNA-binding protein is required for jumbo phage infection. Nucleic Acids Res. 52, 4440–4455. https://doi.org/10.1093/nar/gkae216.

12. Chaikeeratisak, V., Khanna, K., Nguyen, K.T., Egan, M.E., Enustun, E., Armbruster, E., Lee, J., Pogliano, K., Villa, E., and Pogliano, J. (2022). Subcellular organization of viral particles during maturation of nucleus-forming jumbo phage. Sci. Adv. 8, eabj9670. https://doi.org/10.1126/sciadv.abj9670.

13. Danis-Wlodarczyk, K., Vandenheuvel, D., Jang, H.B., Briers, Y., Olszak, T., Arabski, M., Wasik, S., Drabik, M., Higgins, G., Tyrrell, J., et al. (2016). A proposed integrated approach for the preclinical evaluation of phage therapy in Pseudomonas infections. Sci. Rep. 6, 28115. https://doi.org/10.1038/srep28115.

14. Li, Y., Guan, J., Hareendranath, S., Crawford, E., Agard, D.A., Makarova, K.S., Koonin, E.V., and Bondy-Denomy, J. (2022). A family of novel immune systems targets early infection of nucleus-forming jumbo phages. Preprint at bioRxiv. https://doi.org/10.1101/2022.09.17.508391.

15. Guan, J., Oromí-Bosch, A., Mendoza, S.D., Karambelkar, S., Berry, J.D., and Bondy-Denomy, J. (2022). Bacteriophage genome engineering with CRISPR–Cas13a. Nat. Microbiol. 7, 1956–1966. https://doi.org/10.1038/s41564-022-01243-4.

16. Antonova, D., Belousova, V.V., Zhivkoplias, E., Sobinina, M., Artamonova, T., Vishnyakov, I.E., Kurdyumova, I., Arseniev, A., Morozova, N., Severinov, K., et al. (2023). The Dynamics of Synthesis and Localization of Jumbo Phage RNA Polymerases inside Infected Cells. Viruses 15, 2096. https://doi.org/10.3390/v15102096.

17. Danilova, Y.A., Belousova, V.V., Moiseenko, A.V., Vishnyakov, I.E., Yakunina, M.V., and Sokolova, O.S. (2020). Maturation of Pseudo-Nucleus Compartment in P. aeruginosa, Infected with Giant phiKZ Phage. Viruses 12, 1197. https://doi.org/10.3390/v12101197.

18. Reilly, E.R., Abajorga, M.K., Kiser, C., Mohd Redzuan, N.H., Haidar, Z., Adams, L.E., Diaz, R., Pinzon, J.A., Hudson, A.O., Black, L.W., et al. (2020). A Cut above the Rest: Characterization of the Assembly of a Large Viral Icosahedral Capsid. Viruses 12, 725. https://doi.org/10.3390/v12070725.

19. Armbruster, E.G., Lee, J., Hutchings, J., VanderWal, A.R., Enustun, E., Adler, B.A., Aindow, A., Deep, A., Rodriguez, Z.K., Morgan, C.J., et al. (2023). Sequential membrane- and protein-bound organelles compartmentalize genomes during phage infection. Preprint at bioRxiv. https://doi.org/10.1101/2023.09.20.558163.

20. Krylov, V.N., and Zhazykov, I.Zh. (1978). Pseudomonas bacteriophage phiKZ–possible model for studying the genetic control of morphogenesis. Genetika 14, 678–685.

21. Krylov, V.N., Smirnova, T.A., Minenkova, I.B., Plotnikova, T.G., Zhazikov, I.Z., and Khrenova, E.A. (1984). Pseudomonas bacteriophage contains an inner body in its capsid. Can. J. Microbiol. 30, 758–762. https://doi.org/10.1139/m84-116.

22. Wu, W., Thomas, J.A., Cheng, N., Black, L.W., and Steven, A.C. (2012). Bubblegrams Reveal the Inner Body of Bacteriophage φKZ. Science *335*, 182. https://doi.org/10.1126/science.1214120.

23. Thomas, J.A., Weintraub, S.T., Wu, W., Winkler, D.C., Cheng, N., Steven, A.C., and Black, L.W. (2012). Extensive proteolysis of head and inner body proteins by a morphogenetic protease in the giant Pseudomonas aeruginosa phage φKZ. Mol. Microbiol. *84*, 324–339. https://doi.org/10.1111/j.1365-2958.2012.08025.x.

24. Fossati, A., Mozumdar, D., Kokontis, C., Mèndez-Moran, M., Nieweglowska, E., Pelin, A., Li, Y., Guo, B., Krogan, N.J., Agard, D.A., et al. (2023). Next-generation proteomics for quantitative Jumbophage-bacteria interaction mapping. Nat. Commun. *14*, 5156. https://doi.org/10.1038/s41467-023-40724-w.

25. Vida, T.A., and Emr, S.D. (1995). A new vital stain for visualizing vacuolar membrane dynamics and endocytosis in yeast. J. Cell Biol. *128*, 779–792. https://doi.org/10.1083/jcb.128.5.779.

26. Antonova, D., Nichiporenko, A., Sobinina, M., Vishnyakov, I.E., Moiseenko, A., Kurdyumova, I., Khodorkovskii, M., Sokolova, O.S., and Yakunina, M.V. (2024). Genomic Transfer via Membrane Vesicle: A Strategy of Giant Phage phiKZ for Early Infection. Preprint at bioRxiv. https://doi.org/10.1101/2023.12.31.573766.

27. Wicke, L., Ponath, F., Coppens, L., Gerovac, M., Lavigne, R., and Vogel, J. (2021). Introducing differential RNA-seq mapping to track the early infection phase for Pseudomonas phage φKZ. RNA Biol. *18*, 1099–1110. https://doi.org/10.1080/15476286.2020.1827785.

28. Gerovac, M., Chihara, K., Wicke, L., Böttcher, B., Lavigne, R., and Vogel, J. (2024). Phage proteins target and co-opt host ribosomes immediately upon infection. Nat. Microbiol. *9*, 787–800. https://doi.org/10.1038/s41564-024-01616-x.

29. Teo, G., Liu, G., Zhang, J., Nesvizhskii, A.I., Gingras, A.-C., and Choi, H. (2014). SAINTexpress: improvements and additional features in Significance Analysis of Interactome software. J. Proteomics *100*, 37–43. https://doi.org/10.1016/j.jprot.2013.10.023.

30. Yu, F., Teo, G.C., Kong, A.T., Fröhlich, K., Li, G.X., Demichev, V., and Nesvizhskii, A.I. (2023). Analysis of DIA proteomics data using MSFragger-DIA and FragPipe computational platform. Nat. Commun. *14*, 4154. https://doi.org/10.1038/s41467-023-39869-5.

31. Zimmermann, L., Stephens, A., Nam, S.-Z., Rau, D., Kübler, J., Lozajic, M., Gabler, F., Söding, J., Lupas, A.N., and Alva, V. (2018). A Completely Reimplemented MPI Bioinformatics Toolkit with a New HHpred Server at its Core. J. Mol. Biol. *430*, 2237–2243. https://doi.org/10.1016/j.jmb.2017.12.007.

32. Madeira, F., Pearce, M., Tivey, A.R.N., Basutkar, P., Lee, J., Edbali, O., Madhusoodanan, N., Kolesnikov, A., and Lopez, R. (2022). Search and sequence analysis tools services from EMBL-EBI in 2022. Nucleic Acids Res. *50*, W276–W279. https://doi.org/10.1093/nar/gkac240.

33. Perez-Riverol, Y., Csordas, A., Bai, J., Bernal-Llinares, M., Hewapathirana, S., Kundu, D.J., Inuganti, A., Griss, J., Mayer, G., Eisenacher, M., et al. (2019). The PRIDE database and related tools and resources in 2019: improving support for quantification data. Nucleic Acids Res. *47*, D442–D450. https://doi.org/10.1093/nar/gky1106.

34. Vizcaíno, J.A., Deutsch, E.W., Wang, R., Csordas, A., Reisinger, F., Ríos, D., Dianes, J.A., Sun, Z., Farrah, T., Bandeira, N., et al. (2014). ProteomeXchange provides globally coordinated proteomics data submission and dissemination. Nat. Biotechnol. *32*, 223–226. https://doi.org/10.1038/nbt.2839.

35. Schneider, C.A., Rasband, W.S., and Eliceiri, K.W. (2012). NIH Image to ImageJ: 25 years of Image Analysis. Nat. Methods *9*, 671–675. https://doi.org/10.1038/nmeth.2089.

36. Olivella, R., Chiva, C., Serret, M., Mancera, D., Cozzuto, L., Hermoso, A., Borràs, E., Espadas, G., Morales, J., Pastor, O., et al. (2021). QCloud2: An Improved Cloud-based Quality-Control System for Mass-Spectrometry-based Proteomics Laboratories. J. Proteome Res. *20*, 2010–2013. https://doi.org/10.1021/acs.jproteome.0c00853.

37. Cox, J., and Mann, M. (2008). MaxQuant enables high peptide identification rates, individualized p.p.b.-range mass accuracies and proteome-wide protein quantification. Nat. Biotechnol. *26*, 1367–1372. https://doi.org/10.1038/nbt.1511.

STAR★METHODS

KEY RESOURCES TABLE

REAGENT or RESOURCE	SOURCE	IDENTIFIER
Bacterial strains		
Pseudomonas aeruginosa strain PAO1	Joe Bondy- Denomy Lab	NCBI: NC_002516.2
PAO1 [pHERD30T-PHIKZ089-mNeonGreen]	This study	PHIKZ089: Uniprot ID: Q8SD73
PAO1 [pHERD30T-PHIKZ090-mNeonGreen]	This study	PHIKZ090: Uniprot ID: Q8SD72
PAO1 [pHERD30T-PHIKZ093-mNeonGreen]	Guan et al.[15]	PHIKZ093: Uniprot ID: Q8SD69
PAO1 [pHERD30T-PHIKZ095-mNeonGreen]	This study	PHIKZ095: Uniprot ID: Q8SD67
PAO1 [pHERD30T-PHIKZ097-mNeonGreen]	This study	PHIKZ097: Uniprot ID: Q8SD65
PAO1 [pHERD30T-PHIKZ162-mNeonGreen]	This study	PHIKZ162: Uniprot ID: Q8SD00
PAO1 [pHERD30T-PHIKZ093-3xFLAG]	Fossati et al.[24]	PHIKZ093: Uniprot ID: Q8SD69
PAO1 [pHERD30T-PHIKZ093C (PHIKZ093 D157-K435)-3xFLAG]	This study	PHIKZ093: Uniprot ID: Q8SD69
PAO1 [pHERD30T-mNeonGreen-3xFLAG]	This study	N/A
PAO1 [pHERD30T-PHIKZ014-sfCherry2]	This study	PHIKZ014: Uniprot ID: Q8SDE8
PAO1 [pHERD30T-PHIKZ016-sfCherry2]	This study	PHIKZ016: Uniprot ID: Q8SDE6
PAO1 [pHERD30T-PHIKZ022-sfCherry2]	This study	PHIKZ022: Uniprot ID: Q8SDE0
PAO1 [pHERD30T-PHIKZ038-sfCherry2]	This study	PHIKZ038: Uniprot ID: Q8SDC4
PAO1 [pHERD30T-PHIKZ092-sfCherry2]	This study	PHIKZ092: Uniprot ID: Q8SD70
PAO1 [pHERD30T-PHIKZ097-sfCherry2]	This study	PHIKZ097: Uniprot ID: Q8SD65
PAO1 [pHERD30T-PHIKZ174-sfCherry2]	This study	PHIKZ174: Uniprot ID: Q8SCY8
PAO1 [pHERD30T-PHIKZ216-sfCherry2]	This study	PHIKZ216: Uniprot ID: Q8SCU6
PAO1 [pHERD30T-PHIKZ238-sfCherry2]	This study	PHIKZ238: Uniprot ID: Q8SCS4
PAO1 [pHERD30T-PHIKZ238.2-sfCherry2]	This study	PHIKZ238.2: Uniprot ID: L7T0M4
PAO1 [pHERD30T-PHIKZ260-sfCherry2]	This study	PHIKZ260: Uniprot ID: Q8SCQ2
PAO1 [pHERD30T-PHIKZ280-sfCherry2]	This study	PHIKZ280: Uniprot ID: Q8SCN2
PAO1 [pHERD30T-DAVT_PSEAE-sfCherry2]	This study	DAVT: Uniprot ID: Q9I6M4
PAO1 [pHERD30T-LTAE_PSEAE-sfCherry2]	This study	LTAE: Uniprot ID: Q9HTF1
PAO1 [pHERD30T-NADE_PSEAE-sfCherry2]	This study	NADE: Uniprot ID: Q9HUP3
PAO1 [pHERD30T-CARB_PSEAE-sfCherry2]	This study	CARB: Uniprot ID: P38100
PAO1 [pHERD30T-GAPA_PSEAE-sfCherry2]	This study	GAPA: Uniprot ID: P27726
PAO1 [pHERD30T-GYRA_PSEAE-sfCherry2]	This study	GYRA: Uniprot ID: P48372
PAO1 [pHERD30T-HTPG_PSEAE-sfCherry2]	This study	HTPG: Uniprot ID: Q9I3C5
PAO1 [pHERD30T-FABV_PSEAE-sfCherry2]	This study	FABV: Uniprot ID: Q9HZP8
PAO1 [pHERD30T-PORD_PSEAE-sfCherry2]	This study	PORD: Uniprot ID: P32722
PAO1 [pHERD30T-PILM_PSEAE-sfCherry2]	This study	PILM: Uniprot ID: G3XD28
PAO1 [pHERD30T-ETFA_PSEAE-sfCherry2]	This study	ETFA: Uniprot ID: Q9HZP7
PAO1 [pHERD30T-PILA_PSEAE-sfCherry2]	This study	PILA: Uniprot ID: P04739
PAO1 [pHERD30T-sfCherry2]	Mendoza et al.[3]	SDM222
PAO1 [pHERD30T-mNeonGreen-PHIKZ054]	This study	PHIKZ054: Uniprot ID: Q8SDA8
PAO1 [pHERD30T-PHIKZ149-sfCherry2]	This study	PHIKZ149: Uniprot ID: Q8SD13
PAO1 [pHERD30T-PHIKZ180-sfCherry2]	This study	PHIKZ180: Uniprot ID: Q8SCY2
PAO1 [pHERD30T-PHIKZ050-sfCherry2]	This study	PHIKZ050: Uniprot ID: Q8SDB2
PAO1 [pHERD30T-PHIKZ082-sfCherry2]	This study	PHIKZ082: Uniprot ID: Q8SD80
PAO1 [pHERD30T-PHIKZ075-sfCherry2]	This study	PHIKZ075: Uniprot ID: Q8SD87
PAO1 [pHERD30T-sfCherry2-HsdR]	Mendoza et al.[3]	SDM223
PAO1 [pHERD30T-EcoRI-sfCherry2]	Mendoza et al.[3]	SDM248

(Continued on next page)

Continued

REAGENT or RESOURCE	SOURCE	IDENTIFIER
PAO1 [pHERD30T-sfCherry2-Cas3]	Mendoza et al.[3]	N/A
PAO1 [pHERD30T-sfCherry2-Cas8]	Mendoza et al.[3]	N/A
Bacteriophages		
P. aeruginosa bacteriophage ΦKZ	Alan Davidson Lab[20]	NCBI: NC_004629.1
P.aeruginosa bacteriophage ΦPA3	David Agard Lab[2]	NCBI: NC_028999.1
Pseudomonas aeruginosa bacteriophage ΦKZ:gp93-mNeonGreen (genomic fusion)	Guan et al.[15]	N/A
ΦKZ: gp089-mNeonGreen (exogenously packaged)	This study	N/A
ΦKZ: gp090-mNeonGreen (exogenously packaged)	This study	N/A
ΦKZ: gp093-mNeonGreen (exogenously packaged)	Guan et al.[15]	N/A
ΦKZ: gp095-mNeonGreen (exogenously packaged)	This study	N/A
ΦKZ: gp097-mNeonGreen (exogenously packaged)	This study	N/A
ΦKZ: gp162-mNeonGreen (exogenously packaged)	This study	N/A
ΦKZ: gp93-mNeonGreen (genomic fusion) gp092-sfCherry2 (exogenously packaged)	This study	N/A
ΦKZ: gp93-mNeonGreen (genomic fusion) gp097-sfCherry2 (exogenously packaged)	This study	N/A
ΦKZ: gp93-mNeonGreen (genomic fusion) gp174-mNeonGreen (exogenously packaged)	This study	N/A
ΦKZ: gp149-sfCherry2 (exogenously packaged)	This study	N/A
ΦKZ: gp180-sfCherry2 (exogenously packaged)	This study	N/A
Chemicals and Reagents		
(N-(3-Triethylammoniumpropyl)-4-(6-(4-(Diethylamino) Phenyl) Hexatrienyl) Pyridinium Dibromide (FM4-64)	ThermoFisher	Cat# T13320
(1-(4-Trimethyl ammoniumphenyl)-6-Phenyl- 1,3,5-Hexatriene p-Toluenesulfonate) (TMA-DPH)	ThermoFisher	Cat# T204
4′,6-diamidino-2-phenylindole (DAPI)	Invitrogen	Cat# D1306
Luria Broth (Miller's)	Research Products International (RPI)	Cat# L24400
Magnesium Sulfate salt	RPI	Cat# M24300
Gentamicin sulfate salt	Sigma-Aldrich	Cat# G1264
L-(+)-Arabinose	Sigma-Aldrich	Cat# A3256
Agarose, Molecular Biology Grade	RPI	Cat# A20090
Trizma® base	Sigma-Aldrich	Cat# T4661
Sodium Chloride salt, ACS grade	RPI	Cat# S23025
EDTA Disodium Salt [Ethylenediaminetetra-acetic acid, disodium salt dihydrate]	RPI	Cat# E57020
Nonidet P-40 (NP-40)	RPI	Cat# N59000
cOmplete™, Mini, EDTA-free Protease Inhibitor Cocktail	Millipore-Sigma	Cat# 11836170001
Benzonase	Millipore-Sigma	Cat# 101656
4x Laemmli Sample Buffer	Bio-RAD	Cat# 1610747
Beta-mercaptoethanol/ 2-Mercaptoethanol	Bio-RAD	Cat# 1610710
10x Tris/Glycine/SDS Electrophoresis Buffer	Bio-RAD	Cat# 1610772
PVDF Transfer Membranes, 0.2 μm	ThermoFisher Scientific	Cat# 88520
10x Tris/Glycine Buffer (Western Blots, Native Gels)	Bio-RAD	Cat# 1610771
Methanol ACS Grade (99.8%)	Fisher Scientific	Cat# A412-4
Omniblock dry milk powder, non-fat	RPI	Cat# M17200
Tween™ 20 Surfact-Amps™ Detergent Solution	ThermoFisher Scientific	Cat# PI85114
Mouse anti-FLAG M2 antibody	Sigma-Aldrich	Cat# F1804; RRID: AB_262044

(Continued on next page)

Continued

REAGENT or RESOURCE	SOURCE	IDENTIFIER
Purified anti-E. coli RNA Polymerase β Antibody	Biolegend	Cat# 663905; RRID: AB_2566583
Goat anti-mouse HRP	Invitrogen	Ref: 62-6520; Lot: XD347166; RRID: AB_2533947
Clarity Western ECL substrate	Bio-RAD	Cat# 1705061
Anti-Flag M2 Magnetic Beads	Sigma-Aldrich	Cat# M8823: RRID: AB_2637089
RapiGest SF Surfactant	Waters	Cat# 186008740
Urea, ACS reagent, 99.0-100.5%	Sigma-Aldrich	Cat# U5128
DTT, 1,4-dithiothreitol	Sigma-Aldrich	Cat# 10197777001
Iodoacetamide	Sigma-Aldrich	Cat# I6125
Trypsin	Promega	Cat# VA900A
Trifluoroacetic acid (TFA)	Sigma-Aldrich	Cat# 8082600026
Formic Acid, 99.0+%, Optima™ LC/MS Grade	Fisher Scientific	Cat# A117-05AMP
Acetonitrile, LC-MS Grade, 99.8%,	Fisher Scientific	Cat# AA47138K2
Ammonium bicarbonate	Millipore Sigma	Cat# A6141
Tris(2-carboxyethyl)phosphine hydrochloride (TCEP)	Millipore Sigma	Cat# 51805-45-9
2-Chloroacetamide	Millipore Sigma	Cat# C0267
Chloroform (HPLC)	Fisher Scientific	Cat# C607-4
Critical Commercial Assays		
NEBuilder® HiFi DNA Assembly Master Mix	New England Biolabs (NEB)	Cat# E2621
Phusion® High-Fidelity PCR Kit	NEB	Cat# E0553
DNA Clean & Concentrator kit	Zymo Research	Cat #D4034
Plasmid Miniprep Kit	Zymo Research	Cat #ZD4037
Deposited Data		
FLAG AP-MS data	This study	Pride partner ProteomeXchange: PXD049415
PHIKZ Time Course MS data	This study	PRide partner ProteomeXchange: PXD050275
PHIKZ SEC-MS data	Fossati[24]	Massive: MSV000091715
Recombinant DNA		
pHERD30T-PHIKZ089-mNeonGreen	This study	PHIKZ089: Uniprot ID: Q8SD73
pHERD30T-PHIKZ090-mNeonGreen	This study	PHIKZ090: Uniprot ID: Q8SD72
pHERD30T-PHIKZ093-mNeonGreen	Guan et al.[15]	PHIKZ093: Uniprot ID: Q8SD69
pHERD30T-PHIKZ095-mNeonGreen	This study	PHIKZ095: Uniprot ID: Q8SD67
pHERD30T-PHIKZ097-mNeonGreen	This study	PHIKZ097: Uniprot ID: Q8SD65
pHERD30T-PHIKZ162-mNeonGreen	This study	PHIKZ162: Uniprot ID: Q8SD00
pHERD30T-PHIKZ093-3xFLAG	Fossati et al.[24]	PHIKZ093: Uniprot ID: Q8SD69
pHERD30T-PHIKZ093C (PHIKZ093 D157-K435)-3xFLAG	This study	PHIKZ093: Uniprot ID: Q8SD69
pHERD30T-mNeonGreen-3xFLAG	This study	N/A
pHERD30T-PHIKZ014-sfCherry2	This study	PHIKZ014: Uniprot ID: Q8SDE8
pHERD30T-PHIKZ016-sfCherry2	This study	PHIKZ016: Uniprot ID: Q8SDE6
pHERD30T-PHIKZ022-sfCherry2	This study	PHIKZ022: Uniprot ID: Q8SDE0
pHERD30T-PHIKZ038-sfCherry2	This study	PHIKZ038: Uniprot ID: Q8SDC4
pHERD30T-PHIKZ092-sfCherry2	This study	PHIKZ092: Uniprot ID: Q8SD70
pHERD30T-PHIKZ097-sfCherry2	This study	PHIKZ097: Uniprot ID: Q8SD65
pHERD30T-PHIKZ174-sfCherry2	This study	PHIKZ174: Uniprot ID: Q8SCY8
pHERD30T-PHIKZ216-sfCherry2	This study	PHIKZ216: Uniprot ID: Q8SCU6
pHERD30T-PHIKZ238-sfCherry2	This study	PHIKZ238: Uniprot ID: Q8SCS4
pHERD30T-PHIKZ238.2-sfCherry2	This study	PHIKZ238.2: Uniprot ID: L7T0M4
pHERD30T-PHIKZ260-sfCherry2	This study	PHIKZ260: Uniprot ID: Q8SCQ2
pHERD30T-PHIKZ280-sfCherry2	This study	PHIKZ280: Uniprot ID: Q8SCN2

Continued

REAGENT or RESOURCE	SOURCE	IDENTIFIER
pHERD30T-DAVT_PSEAE-sfCherry2	This study	DAVT: Uniprot ID: Q9I6M4
pHERD30T-LTAE_PSEAE-sfCherry2	This study	LTAE: Uniprot ID: Q9HTF1
pHERD30T-NADE_PSEAE-sfCherry2	This study	NADE: Uniprot ID: Q9HUP3
pHERD30T-CARB_PSEAE-sfCherry2	This study	CARB: Uniprot ID: P38100
pHERD30T-GAPA_PSEAE-sfCherry2	This study	GAPA: Uniprot ID: P27726
pHERD30T-GYRA_PSEAE-sfCherry2	This study	GYRA: Uniprot ID: P48372
pHERD30T-HTPG_PSEAE-sfCherry2	This study	HTPG: Uniprot ID: Q9I3C5
pHERD30T-FABV_PSEAE-sfCherry2	This study	FABV: Uniprot ID: Q9HZP8
pHERD30T-PORD_PSEAE-sfCherry2	This study	PORD: Uniprot ID: P32722
pHERD30T-PILM_PSEAE-sfCherry2	This study	PILM: Uniprot ID: G3XD28
pHERD30T-ETFA_PSEAE-sfCherry2	This study	ETFA: Uniprot ID: Q9HZP7
pHERD30T-PILA_PSEAE-sfCherry2	This study	PILA: Uniprot ID: P04739
pHERD30T-sfCherry2	Mendoza et al.[3]	pSG30T-cherry
pHERD30T-mNeonGreen-PHIKZ054	This study	PHIKZ054: Uniprot ID: Q8SDA8
pHERD30T-PHIKZ149-sfCherry2	This study	PHIKZ149: Uniprot ID: Q8SD13
pHERD30T-PHIKZ180-sfCherry2	This study	PHIKZ180: Uniprot ID: Q8SCY2
pHERD30T-PHIKZ050-sfCherry2	This study	PHIKZ050: Uniprot ID: Q8SDB2
pHERD30T-PHIKZ082-sfCherry2	This study	PHIKZ082: Uniprot ID: Q8SD80
pHERD30T-PHIKZ075-sfCherry2	This study	PHIKZ075: Uniprot ID: Q8SD87
pHERD30T-sfCherry2-HsdR	Mendoza et al.[3]	pSDM153
pHERD30T-EcoRI-sfCherry2	Mendoza et al.[3]	pSDM171
pHERD30T-sfCherry2-Cas3	Mendoza et al.[3]	pSG30T-cherrycas3(IC)
pHERD30T-sfCherry2-Cas8	Mendoza et al.[3]	pSG30T-cherrycas8(IC)
Softwares and Algorithms		
SAINTexpress (version 3.6.1)	Teo et al.[29]	https://saint-apms.sourceforge.net/Main.html
Fragpipe (version 19.1)	Yu et al.[30]	https://fragpipe.nesvilab.org/
PhageMAP	Fossati et al.[24]	https://phagemap.ucsf.edu/home/
Prism version 10.1.0 (264)	GraphPad Prism	https://www.graphpad.com/
Fiji (Fiji is just ImageJ) (version 2.0.0-rc-69/1.53h)	ImageJ wiki	https://imagej.net
HHPred	Zimmerman et al.[31]	https://toolkit.tuebingen.mpg.de/tools/hhpred
Clustal Omega Multiple Sequence Alignment (MSA)	Madeira et al.[32]	https://www.ebi.ac.uk/jdispatcher/msa/clustalo

RESOURCE AVAILABILITY

Lead contact
Further information and requests for resources and reagents should be directed to and will be fulfilled by the lead contact, Joseph Bondy-Denomy (Joseph.Bondy-Denomy@ucsf.edu).

Materials availability
All unique/stable reagents generated in this study are available from the lead contact with a completed Materials Transfer Agreement.

Data and code availability
The NCBI/ Uniprot accession number for the genes used in this study are listed in the key resources table. The raw data files and search results from mass spectrometry experiments performed in this study are available from the Pride partner ProteomeXchange[33,34] repository under the identifier Pride partner ProteomeXchange: PXD049415 identifier (AP-MS experiments) and Pride partner ProteomeXchange: PXD050275 (time-course MS experiments). The processed proteomics data is available in Data S1 and Data S2 respectively. See STAR Methods section for additional details. SEC-MS data used in this study are available on the website PhageMAP[24] (https://phagemap.ucsf.edu/home/). This paper does not report original code. Any additional information required to reanalyze the data reported in this paper is available from the lead contact upon request.

EXPERIMENTAL MODEL AND SUBJECT DETAILS

Bacterial strains and phages

The bacterial strains and phages used in this study are listed in the key resources table. The *P. aeruginosa* strains (PAO1) and E. coli strains (DH5α) were grown in Luria broth (LB) medium at 37°C both with aeration at 225 r.p.m. Growth media were supplemented with 10 mM MgSO4 when performing phage infections, and when indicated, gentamicin (50 mg ml^{-1} for *P. aeruginosa* and 15 mg ml^{-1} for E. coli) was used to maintain the pHERD30T plasmid. Gene expression was induced by the addition of L-arabinose (0.03% final for bacterial/phage genes, unless otherwise specified).

METHOD DETAILS

Preparation of phages packaged with fluorescent protein (FP)-labeled phage virion protein

This was performed with a previously described procedure.[24] Briefly PAO1 cells expressing mNeonGreen/ sfCherry2 fusions of a given virion protein were infected at mid-log phase (OD 0.5-0.6) with either ΦKZ (WT)/ or ΦKZ: gp93-mNeonGreen (genomic fusion, ref. Guan et al.[15], *Nat. Microbiol*) at MOI =1 on ice (for 10 min to allow complete adsorption) and thereafter at 37°C for 2 hours, at 175 rpm. Thereafter bacterial cells were lysed with chloroform to release phage particles. Phage particles from the cellular lysate were concentrated with an Amicon® Ultra Centrifugal Filter, 100 kDa MWCO to remove excess fluorescent proteins. The concentrated phage fraction was used for subsequent fluorescence microscopy experiments investigating the localization of injected virion proteins.

Fluorescence microscopy and imaging

For studying localization of virion proteins: PAO1 cells (WT)were grown overnight in 3 mL LBM (LB with 10mM MgSO$_4$) (supplemented with gentamicin 50 μg/ml, as appropriate) at 37 °C with aeration at 175 rpm. The overnight culture was diluted 100-fold in 3 ml of LBM (containing 0.03% Arabinose) and grown at 37 °C with 175 r.p.m. shaking to an OD600 of approximately 0.5. Thereafter PAO1 cells (≈1 OD equivalent) were infected with ΦKZ particles (as described in the previous section)(approximate MOI of 1-10) on ice for 10 min (to allow complete adsorption of virions onto cells) and then incubated at 30 °C for indicated times. *For studying localization of non-virion phage/ host proteins*: PAO1 cells expressing sfCherry2 fusions of non-virion phage/ host) were grown overnight in 3 mL LBM (LB with 10mM MgSO$_4$) (supplemented with gentamicin 50 μg/ml, as appropriate) at 37 °C with aeration at 175 rpm. The overnight culture was diluted 100-fold in 3 ml of LBM (containing 0.03% Arabinose) and grown at 37 °C with 175 r.p.m. shaking to an OD600 of approximately 0.5. Thereafter PAO1 cells (≈1 OD equivalent) were infected with ΦKZ particles (WT or genomically expressing gp93-mNeonGreen) (approximate MOI of 1-10) on ice for 10 min (to allow complete adsorption of virions onto cells) and then incubated at 30 °C for indicated times. Thereafter 2 μL of the uninfected/ infected culture was applied onto an was gently placed onto a piece of agarose pad (approximately 1 mm thick) with 1:4 diluted LBM, arabinose (0.8%) and fluorescent dyes namely: 4′,6-diamidino-2-phenylindole (DAPI; 5 μg ml−1; Cat# D1306; Invitrogen) or (N-(3-Triethylammoniumpropyl)-4-(6-(4-(Diethylamino) Phenyl) Hexatrienyl) Pyridinium Dibromide (FM4-64; 5 μg ml−1; Cat# T13320, ThermoFisher) or (1-(4-Trimethyl ammonium-phenyl)-6-Phenyl- 1,3,5-Hexatriene p-Toluenesulfonate) (TMA-DPH; 5 μg ml−1; Cat# T204). A coverslip (no. 1.5; Thermo Fisher Scientific) was gently laid over the agarose pad and the sample was imaged under a fluorescence microscope at 30 °C within a cage incubator to maintain temperature and humidity. Microscopy was performed on an inverted epifluorescence microscope (Ti2-E; Nikon) equipped with the Perfect Focus System and a Photometrics Prime 95B 25-mm camera. Image acquisition and processing were performed with the Nikon Elements AR software v.5.02.00 (64-bit). Specimens were imaged at a time interval through channels of phase contrast (200 ms exposure for cell recognition), blue (DAPI, 200 ms exposure for phage DNA; TMA-DPH, 500 ms exposure), green (mNeonGreen, 5s long exposure for gp93-mNeonGreen) and red (FM4-64, 200ms exposure; sfCherry2, 500ms exposure). All representative fluorescence microscopy images were sourced from at least two independent biological replicates. Images were analyzed with Fiji/ ImageJ (2.0.0-rc-69/1.53h)[35]

Western Blotting

PAO1 cells (WT or expressing gp93-3xFLAG/ mNeonGreen-3xFLAG) were grown overnight in 3 mL LB (supplemented with gentamicin 50 μg/ml, as appropriate) at 37 °C with aeration at 175 rpm. Cells were diluted 1:100 from a saturated overnight culture into 5 mL LB with 10 mM MgSO4 (for WT PAO1), or supplemented with Arabinose (for PAO1: gp93-3xFLAG/ mNeonGreen-3xFLAG) and grown for 2.5 h at 37 °C with aeration at 175 rpm. Upon reaching 0.5 OD (600 nm), gentamicin was added to WT PAO1 cells (50 μg/ml), and the cells were chilled on ice for 5 min. Thereafter (1) WT PAO1 cells (≈1 OD equivalent) were infected with ΦKZ particles packaged with gp93-3xFLAG-tag/ (2) PAO1 cells expressing gp93C-3xFLAG/ mNeonGreen -3xFLAG were infected with WT ΦKZ particles (MOI ≈ 1) on ice for 10 min (to allow complete adsorption of virions onto cells) and then incubated at 30°C for 15 min. Thereafter, the cell cultures were transferred to pre-chilled 15 mL falcon tubes and centrifuged at 6000×g, 4 °C for 5 min. The supernatant was discarded, and the cell pellet was washed twice with 2 mL of pre-chilled (4 °C) LB to remove excess unbound virions. The cell pellet was lysed in 100 μL of lysis buffer (50 mM Tris (pH 7.4), 150 mM NaCl, 1 mM EDTA, 0.5% NP-40, 1x protease inhibitor cocktail (Roche, complete mini EDTA free), 125 U Benzonase/mL). The lysed suspension was further sonicated on ice using a Q125 sonicator (10 pulses, 1 s ON, 1 s OFF, 30% amplitude). The cell lysate was centrifuged at 15,000 × g (15 min, 4 °C) to remove cellular debris. The clarified cellular lysate (100 μL) was boiled with 33 μL of 4x Laemmli Buffer (with Beta-mercaptoethanol) for

10 min. 14 μL of lysate samples were loaded. For virion control samples, 10 μL of purified virions were boiled with 3.3 μLL of 4x Laemmli Buffer (with Beta-mercaptoethanol) for 10 min, and 2 μL of samples were loaded. SDS-PAGE gels were run with running buffer (100 mL 10× Tris-Glycine SDS Buffer, 900 mL Milli-Q water) at 130 V for 1 h (constant voltage setting). The SDS-PAGE gels were transferred onto 0.2 μM PVDF membranes using a wet transfer (Transfer Buffer: 100 mL 10× Tris-Glycine Buffer, 200 mL methanol, 700 mL Milli-Q water; 100 V, 1 hour, 4 °C). The membranes were incubated with a blocking buffer (5% Omniblock milk, non-fat-dry in 1× TBST (200 mL Tris Buffer Saline, 0.20 mL Tween-20)) for 1 h at room temperature. Thereafter the blocking buffer was discarded, and the membranes were incubated with 1:1000 dilutions of mouse anti-FLAG M2 antibody (Sigma-Aldrich, Cat# F1804) or anti-RNAP$_\beta$ antibody (Biolegend, Cat# 663905) in 1×TBST (overnight, 4 °C, with constant shaking). Thereafter the membranes were washed thrice for 10 min with TBST and incubated with 1:3000 dilution of Goat anti-mouse HRP (Ref: 62-6520; Lot: XD347166 Invitrogen) in blocking buffer for 1 hr at room temperature with constant shaking. Finally, the membranes were washed thrice for 10 min with TBST and incubated with Clarity Western ECL substrate. Membranes were imaged on an Azure 500 imager for variable amounts of time. The representative western blots (presented in Figure 1C) were sourced from at least two independent biological replicates.

FLAG AP-MS

Lysate samples of PAO1 cells prepared (prepared exactly as described for western blotting) were used for AP-MS experiments. For FLAG purifications, 30 μL of bead slurry (Anti-Flag M2 Magnetic Beads, Sigma) was washed twice with 1 mL of ice-cold wash buffer (50 mM Tris pH 7.4, 150 mM NaCl, 1 mM EDTA) and the lysate was incubated with the anti-FLAG beads at 4°C with rotation for 2 hrs. After incubation, flow-through was removed and beads were washed once with 500 μL of wash buffer with 0.05% NP40 and twice with 1 mL of wash buffer (no NP40). Bound proteins were eluted by incubating beads with 15 μL of 100 ug/ml 3xFLAG peptide in 0.05% RapiGest in the wash buffer for 15 min at RT with shaking. Supernatants were removed and elution was repeated. Eluates were combined and 10 μL of 8 M urea, 250 mM Tris, 5 mM DTT (final concentration ~1.7 M urea, 50 mM Tris, and 1 mM DTT) was added to give a final total volume of ~45 μL. Samples were incubated at 60°C for 15 min and allowed to cool to room temperature. Iodoacetamide was added to a final concentration of 3 mM and incubated at room temperature for 45 min in the dark. DTT was added to a final concentration of 3 mM before adding 1 μg of sequencing-grade trypsin (Promega) and incubating at 37°C overnight. Samples were acidified to 0.5% TFA (ph<2) with 10% TFA stock and incubated for 30 min before desalting on C18 ultra micro spin columns (The Nest Group). After lyophilization of desalted eluants, samples were resuspended in 20 μL of 0.1% formic acid and 2μL were separated by a reversed-phase gradient from 2.4% acetonitrile in 0.1% formic acid to 22.4% acetonitrile over the course of 44 min, followed by a 5 min ramp to 36% acetonitrile, and a final column wash at 70.4% acetonitrile for 10 min. Separations were performed using a nanoflow 75μm ID x 25cm long picotip column packed with 1.9μM C18 particles (Dr. Maisch). Peptides were directly injected over the course of a 60 min acquisition into an Orbitrap Fusion Lumos Tribrid Mass Spectrometer (Thermo) and MS1 scans were collected in the orbitrap, while MS2 was performed with HCD fragmentation and data collection in the ion trap. Instrument performance was monitored by QCloud 2.0.[36] Raw MS data were searched against both the ΦKZ and the and the PAO1 proteomes, and using the default settings in MaxQuant (version 2.0.3.0).[37] Peptides and proteins were filtered to 1% false discovery rate in MaxQuant, and identified proteins spectral counts were then subjected to protein-protein interaction scoring with SAINTexpress (version 3.6.1),[29] using both the gp93cyto and the mNeongreen-3xFlag as negative controls. All raw data files and search results are available from the Pride partner ProteomeXchange repository under the PXD049415 identifier.[33,34] reviewer_pxd049415@ebi.ac.ukThe processed FLAG AP-MS proteomics data is presented in Data S1. The FLAG AP-MS data for all samples was sourced from three independent biological replicates.

Time Course MS

Mid-log cultures of PAO1 cells (OD 0.5-0.6, 50 mL) were infected with WT ΦKZ particles (MOI ≈ 1) on ice for 10 min (to allow complete adsorption of virions onto cells) and then incubated at 30 °C for 10 and 20 min respectively. Cultures of infected cells were flash frozen on liquid nitrogen and subsequently mechanically lysed using a SPEX-freezer mill (cryo-milling). Powdered lysate samples were resuspended in Urea lysis buffer (8M urea, 100 mM ammonium bicarbonate pH 8) supplemented with a Complete protease inhibitor tablet (Roche). Samples were centrifuged at 13'000 rpm for 10 minutes to remove cellular debris.

Protein amount was assessed by BCA and approximately ~50 ug per sample were used per replicate.

TCEP was added to 5 mM final concentration and samples were incubated at 25 C for 30 minutes on a shaker (400 rpm), reduced cysteines were alkylated with 10 mM chloroacetamide for 1 hr in the dark at 25 C.

Urea concentration was reduced to 1 M by addition of 100 mM ammonium bicarbonate pH 8. 1 ug of trypsin was added per sample and proteins were digested overnight at 30 C on a thermo shaker (400 rpm).

The next day, samples were acidified with 20% TFA to pH ~2 and desalting was performed as previously described for AP-MS. The MS acquisition was performed on an Orbitrap Exploris operating in DDA mode interfaced with a Vanquish Neo HPLC. The samples were separated in 70 minutes of a linear gradient from 5 to 37% B (0.1% FA in ACN) followed by 10 minutes at 90% B and 5 minutes to equilibrate the column at 5% B. The MS samples were searched against a protein database composed of phiKZ (refSeq id: NC_004629) and PAO1 (6026 entries in total) in Fragpipe (v19.1) using the 'LFQ-MBR' workflow with default parameters. The normalized spectral counts for all phage proteins at individual time points (presented in Figure 4B) was computed as the ratio of unique spectral counts with protein length. All raw data files and search results from this experiment are available from the Pride partner ProteomeXchange repository under the PXD050275 identifier.[33,34] The processed

Time-Course MS proteomics data is presented in Data S1. The time course MS data for all samples was sourced from three independent biological replicates.

SEC-MS

SEC-MS data is derived from experiments performed for a prior publication.[24] Graphs displaying elution profiles of individual proteins were generated with Graphpad Prism.

Bioinformatic Analysis

Paralogous domains presented in Figure S1B were assigned based on an HHPred search against the Pfam-A_v36 database (https://toolkit.tuebingen.mpg.de/tools/hhpred). Pairwise sequence identity measurements of the reported paralogous domains presented in Figure S1C, were made use the Clustal Omega Multiple Sequence Alignment (MSA) server (https://www.ebi.ac.uk/jdispatcher/msa/clustalo)

QUANTIFICATION AND STATISTICAL ANALYSES

All quantification and statistical analyses performed on the proteomics data (AP-MS: Figures 1D and 2A & Time-course MS: Figure 4B) are detailed in the STAR Methods section of this manuscript. For all proteomics experiments, the primary data was sourced for three independent biological replicates. Quantification/ statistical analyses of western blotting/ fluorescence microscopy experiments were not performed. The representative western blots (Figure 1C) and fluorescence microscopy images (Figures 1E, 2B–2D, 3A–3H, 4A, 4D, 4E, S1A, and S2–S4) presented in this paper were sourced from at least two independent biological replicates. Details of all bioinformatic analyses performed are listed in the STAR Methods section of the paper.

ADDITIONAL NOTES

Note that microscopy data appearing in Supplementary Figure S1A previously appeared in a preprint (https://doi.org/10.1101/2022.09.17.508391) from our lab. These data have been removed from the Li et al.[15] manuscript and used here instead. The Li manuscript has been updated and these data will not appear in the final published paper.